Physica B xxx (xxxx) xxx–xxx

Contents lists available at ScienceDirect

Physica B

journal homepage: www.elsevier.com/locate/physb

Impurity effects in the magnetic oscillations on doped graphene with Zeeman splitting

F. Escudero[a], J.S. Ardenghi[b,*], Paula Jasen[b], A. Juan[b]

[a] Departamento de Física, Universidad Nacional del Sur, Av. Alem 1253, B8000CPB Bahía Blanca, Argentina
[b] Instituto de Física del Sur (IFISUR, UNS-CONICET), Av. Alem 1253, B8000CPB Bahía Blanca, Argentina

ARTICLE INFO

Keywords:
Graphene
Zeeman effect
Disorder
De Haas-van Alphen oscillations

ABSTRACT

The aim of this work is to describe the electronic and magnetic properties of graphene in a constant magnetic field, in the long wavelength approximation with random disorder. Taking into account the Zeeman effect, the electronic density of states for each spin is found and the de Haas van Alphen oscillations (dHvA) are found. The magnetic field is found to modulate the de Haas-van Alphen magnetization through the ratio of the Zeeman coupling and pseudospin-Landau coupling. In turn, the Pauli magnetization is studied showing that the Zeeman splitting and disorder introduces a dHvA oscillation period that depends on the magnetic field strength and generalizes the Onsager relation. In turn, a beat frequency appears that does not depend on B but increase linearly with the chemical potential. These results, which are different from those obtained in the standard nonrelativistic 2D electron gas, are attributed to its anomalous Landau level spectrum in graphene.

1. Introduction

Since its experimental isolation in 2004, graphene has become one of the most studied and promising material in solid state physics ([1–3]). Its interesting properties lie in his 2D hexagonal structure, made of two interpenetrating sublattices A and B that act as a pseudospin degrees of freedom [4]. With no impurities or defects, the conduction and valence bands touch at two inequivalent points at the corners of the Brillouin zone with the valence band full and the conduction band empty in the ground state [3]. Furthermore, in pristine graphene the density of states at the Fermi energy is zero, and thus the graphene is a semiconductor with zero band gap, or a semi-metal [5]. When a magnetic field is applied to graphene, discrete Landau levels are obtained [6] and these are not equidistant, as in classical electron gas. In turn, the large distance between the fundamental and first excited Landau levels allows the Quantum Hall effect to be observed in graphene at room temperatures ([7–9]). Moreover, the Landau levels create an oscillating behavior in the thermodynamics potentials. It is found that the magnetization oscillates as a function of the inverse magnetic field, the so called de Haas van Alphen effect (dHvA) ([10,11]). The different frequencies involved in the oscillations are related to the closed orbits that electrons perform on the Fermi surface [12] and is a powerful tool for mapping the electronic states at the Fermi energy [13]. It has been predicted in graphene that magnetization oscillates periodically in a sawtooth pattern, in agreement with the old Peierls prediction [14], although the basic aspects of the behavior of the magnetic oscillations for quasi-2D materials remains yet unclear [15]. In contrast to 2D conventional semiconductors, where the oscillating center of the magnetization M remains exactly at zero, in graphene the oscillating center has a positive value because the diamagnetic contribution is half reduced with that in the conventional semiconductor [16]. From an experimental point of view, carbon-based materials are more promising because the available samples already allows one to observe the Shubnikov-de Haas effect ([17,18]) and then may be easier to interpret the quantum oscillations in its transport properties. Because the dHvA signal in 2D systems are free of the k_z smearing, it should be easier to obtain much rich information about the electron processes. On the other side, it is well known that pristine graphene is ideal. Real world samples of graphene are essentially impure, as they always contain some amount of resonant impurities or ripples. Considering pristine graphene, these defects can break the pseudospin symmetries, depending on the matrix elements in the external potential [19]. The problem of scattering from subtitutional impurities in the presence of a magnetic field does not have yet a satifactory solution, although it is known that broadening of Landau levels in the electronic density of states is good approximation valid in weak magnetic fields [20]. This broadening has the technical advantage that if one consider first the dHvA oscillations with Dirac delta shaped Landau levels, the introduction of impurities implies to convolute the different quantities of interest with the appropriate distribution func-

* Corresponding author.
E-mail address: jsardenghi@gmail.com (J.S. Ardenghi).

http://dx.doi.org/10.1016/j.physb.2017.05.012
Received 12 March 2017; Received in revised form 3 May 2017; Accepted 7 May 2017

tions [14]. However, this is a simplification that is only valid if all the Landau levels have the same width. To obtain better theoretical approximations in this work the Born approximation will be used to compute the self-energies [21]. This work will be organized as follow: In section II, the magnetic Green function with diagonal on-site energies will be computed for graphene. In section III, single-site approximation will be applied and a system of coupled Soven equation will be found and solved. The discussion of the results is shown in section IV and the principal findings of this paper are highlighted in the conclusion. In Appendix the main theory used in the manuscript is explained.

2. Single-site approximation

For a self-contained lecture of this paper, the self-consistent Born approximation will be explained in this section in order to obtain the generalization to the results obtained in [22], Eq. (68) to Eq. (72). The Hamiltonian in the two inequivalent corners of the Brillouin zone in the long wavelength approximation reads

$$H = v_F \begin{pmatrix} 0 & \pi_x - i\pi_y & 0 & 0 \\ \pi_x + i\pi_y & 0 & 0 & 0 \\ 0 & 0 & 0 & \pi_x + i\pi_y \\ 0 & 0 & \pi_x - i\pi_y & 0 \end{pmatrix} \tag{1}$$

where $\pi_i = p_i - eA_i$, being A_i the vector potential. This approximation holds for $E < E_C$ where $E_C = v_F k_C \sim t \sim 2.7\, eV$ (see [22] above eq. (24)). By considering that $\mathbf{A} = (-By, 0, 0)$ and by writing the wave function as $\psi = e^{ikx}\phi(y)$, then p_x transform as $p_x \to \hbar k$. By making the following transformation $y = \frac{\hbar}{\sqrt{eB}}\overline{y} + \frac{\hbar k_x}{eB} = l_B\overline{y} + kl_B^2$, the last Hamiltonian can be written as

$$H_0 = v_F\sqrt{2eB\hbar}\begin{pmatrix} 0 & a^\dagger & 0 & 0 \\ a & 0 & 0 & 0 \\ 0 & 0 & 0 & a \\ 0 & 0 & a^\dagger & 0 \end{pmatrix} \tag{2}$$

where $a = \frac{1}{\sqrt{2}}(\overline{y} + \partial_{\overline{y}})$ and $a^\dagger = \frac{1}{\sqrt{2}}(\overline{y} - \partial_{\overline{y}})$. This Hamiltonian can be written in terms of two copies of identical valley Hamiltonians

$$H_0 = \hbar\omega_L(\sigma_+ a^\dagger + \sigma_- a) \otimes \hbar\omega_L(\sigma_- a^\dagger + \sigma_+ a) \tag{3}$$

where $\sigma_\pm = \sigma_x \pm i\sigma_y$ acts on the sublattice basis and where $\omega_L = v_F\sqrt{\frac{eB}{2\hbar}}$ is the cyclotron frequency. The tensor product is introduced to denote the valley subspaces. In order to simplify the problem, we can consider only the K valley. Because the magnetic field can interact with the spin of electrons, then we can add the Zeeman Hamiltonian by adding the spin space. Then, the Hamiltonian will be a 2×2 block diagonal matrix, where the first block is for spin up and the second block for spin down, both for the same K valley.[1] The wave function can be written as

$$|\psi_{k,n}\rangle = \begin{pmatrix} c_1|k, n\rangle \\ c_2|k, n-1\rangle(1-\delta_{n,0}) \\ c_3|k, n\rangle \\ c_4|k, n-1\rangle(1-\delta_{n,0}) \end{pmatrix} \tag{4}$$

where the coordinate representation of $|k, n\rangle$ is $\langle r|k, n\rangle = e^{ikx}\phi_{n,k}(\overline{y})$, where $\phi_{n,k}(\overline{y})$ is the wave function of the harmonic oscillator.[2]

$$\phi_{n,k}(\overline{y}) = \frac{\pi^{-1/4}}{\sqrt{2^n n!}} e^{-\frac{1}{2}\overline{y}^2} H_{n,k}(\overline{y}) \tag{5}$$

and where $H_{n,k}(\overline{y})$ are the Hermite polynomials. After straightforward manipulations, the eigen problem reduces to

$$\begin{pmatrix} -\hbar\omega_z & \hbar\omega_L\sqrt{n} & 0 & 0 \\ \hbar\omega_L\sqrt{n} & -\hbar\omega_z & 0 & 0 \\ 0 & 0 & \hbar\omega_z & \hbar\omega_L\sqrt{n} \\ 0 & 0 & \hbar\omega_L\sqrt{n} & \hbar\omega_z \end{pmatrix}\begin{pmatrix} c_1 \\ c_2 \\ c_3 \\ c_4 \end{pmatrix} = E\begin{pmatrix} c_1 \\ c_2 \\ c_3 \\ c_4 \end{pmatrix} \tag{6}$$

Then, the eigenvalues can be written as

$$\epsilon_n^{(\alpha,s)} = -s\hbar\omega_Z + \alpha\hbar\omega_L\sqrt{n} \tag{7}$$

where $\alpha = +1(-1)$ for the conduction (valence band), $s = +1(-1)$ for the spin up (spin down). The eigenfunctions read

$$|\psi_{k,n,s,\alpha}\rangle = \frac{1}{\sqrt{(2-\delta_{n,0})L}}\begin{pmatrix} \frac{\alpha}{2}(1+s)|k, n\rangle \\ -\frac{1}{2}(1+s)|k, n-1\rangle(1-\delta_{n,0}) \\ \frac{\alpha}{2}(s-1)|k, n\rangle \\ \frac{1}{2}(s-1)|k, n-1\rangle(1-\delta_{n,0}) \end{pmatrix} \tag{8}$$

where $L^2 = A$, where A is the area of the graphene sheet. In the basis that diagonalize the Hamiltonian, the Green function reads

$$G_0 = \sum_{\alpha=\pm 1, s=\pm 1}\sum_{k,n}\frac{1}{z - \epsilon_n^{(\alpha,s)}}|\psi_{k,n,s,\alpha}\rangle\langle\psi_{k,n,s,\alpha}| \tag{9}$$

where z is a complex number that can be written as $z = E + is$, where E is the energy and s is some real and positive number. At this point we can include disorder as random impurities in our model in the most simple way in order to gain a physical understanding of its effects. By considering an impurity potential in the coordinate representation (see Eq. (59) of [22]) $V(r) = V_0\sum_N^{i=1}\delta(r - R_i)I$, where R_i are the random positions of the impurities and I is the identity matrix, it can be shown that when configurational averaging is applied over the random positions of the impurities, the system restore translation invariance and the configurational averaged Green function $\langle G\rangle$ can be written in terms of the self-energy (see [24])

$$\langle G(k, z)\rangle = [G_0^{-1}(k) - \Sigma(k, z)]^{-1} \tag{10}$$

where $\langle\ldots\rangle$ means configurational averaging. In turn, it can be shown that in the self-consistent Born approximation, the self-energy at first order in the impurity concentration $c = N_i/N$ can be written as (see [24] eq.(3.59))

$$\Sigma^{SCBA}(z) = cV_0^2\sum_k\langle G(k)\rangle \tag{11}$$

where we are neglecting skeleton diagrams where impurity lines crosses and the sum in k represent the sum in all the quantum numbers of the system. In the case of graphene with magnetic field, our Hamiltonian depends on the momentum k in the x direction, the n label of the Landau levels, the spin and conduction and valence band. If we consider the sum over the Landau levels and k then last equation becomes

$$\Sigma_{\alpha,s}(z) = cV_0^2\int\frac{dk}{2\pi}\sum_{n=0}^{Q}G(\alpha, s, n, k, z) \tag{12}$$

where the self-energy depends on the conduction-valence band and spin and Q is the Landau level cutoff that is determined by the equation $\hbar\omega_Z + \hbar\omega_L\sqrt{Q} = E_C$. The impurity-averaged Green function $\langle G(\alpha, s, n, k, z)\rangle$ can be written in the spectral representation as[3]

$$\langle G(\alpha, s, n, k, z)\rangle = \frac{1}{(2-\delta_{n,0})}\frac{1}{z - \epsilon_n^{(\alpha,s)} - \Sigma_{\alpha,s}(z)} \tag{13}$$

where we have introduced the self-energy diagonal matrix elements $\Sigma_{\alpha,s}(z)$. Eq. (12) contains four independent self-consistent equations for the self-energies. Nevertheless, by following Eq. (11) we must sum over

[1] Other effects such as spin-orbit coupling has been considered (see [23]), where the spin-orbit coupling can be tuned by electric fields.

[2] The factor $(1-\delta_{n,0})$ is introduced to discriminate the ground state which contributes only in the A sublattice for the K valley. If we had considered the K' valley, the contribution is on the Bsublattice.

[3] In order to apply Eq. (10), the self-energy is considered diagonal in the spectral representation.

the remaining indices α and s. Summing in α, we obtain two spin dependent self-energies equations

$$\Sigma_s(z) = cV_0^2 D \sum_{n=0}^{Q} \frac{1}{2-\delta_{n,0}} \frac{2(z - s\hbar\omega_z - \Sigma_s(z))}{(z - s\hbar\omega_Z - \Sigma_s(z))^2 - \hbar^2\omega_L^2 n} \tag{14}$$

By performing the sum in n, last equation reads

$$\sigma_s = 2cv^2 D(\epsilon + s\eta - \sigma_s) \sum_{n=0}^{Q} \frac{1}{(\epsilon - s\eta - \sigma_s)^2 - n} \tag{15}$$

where $\sigma_s = \frac{\Sigma_s}{\hbar\omega_L}$, $v = \frac{V_0}{\hbar\omega_L}$, $\eta = \frac{\omega_z}{\omega_L}$ and $\bar{z} = \frac{z}{\hbar\omega_L} = \epsilon$ are all dimensionless variables and where $\epsilon = \frac{E}{\hbar\omega_L}$. The dimensionless averaged Green function, now denoted as $g(\bar{z})$ reads

$$g(\bar{z}) = \sum_{s,\alpha,n} \frac{1}{\bar{z} + s\eta - \alpha\sqrt{n} - \sigma_s} \tag{16}$$

where $g(\bar{z}) = \hbar\omega_L G(z)$ and $G(z) = \sum_{s,n,\alpha} \langle G(\alpha, s, n, k, z)\rangle$. The total density of states can be computed as $\rho(\epsilon) = -\frac{1}{\pi}\Im g(\bar{z})$. The typical values for the couplings are $\hbar\omega_L \sim 36.29\sqrt{B[T]}meV$ and $\hbar\omega_Z \sim 0.1B[T]meV$ (see [25,26]), then $\eta \sim 0.0027\sqrt{B}$, which for typical values of B implies $\eta < 1$. As a brief example of Eq. (15) we can consider an extreme particular and artificial case in which $Q = (\epsilon_c - \eta)^2 = 0$. where $\epsilon_C = E_C/\hbar\omega_L$, which implies that there is a unique Landau $\frac{1}{z + s\hbar\omega_z - \alpha\hbar\omega_L - \Sigma_s}$ level for each spin. The magnetic field strength that obeys Q=0 is such that $\eta = \epsilon_C$ which implies a non-feasible magnetic field strength in the laboratory, but it can give insight in the way the self-energy affects the clean density of states. By using Eq. (15), the self-energy can be computed exactly from the following equation

$$\sigma_s = \frac{2cv_0^2 D}{\epsilon + s\eta - \sigma_s} \tag{17}$$

and the solution reads

$$\sigma_s = \frac{\epsilon + s\eta \pm \sqrt{(\epsilon + s\eta)^2 - 8cv_0^2 D}}{2} \tag{18}$$

Last result is similar to the self-energy of the Falicov-Kimball model without static disorder(see [27]). There are two possible solutions for σ_s given by the sign of the third term of last equation and we have to select the one with the correct analytic properties. Because the possible imaginary part of σ_s originates in the square root term, then by using Eq. (18) we must consider only the negative solution. By introducing σ_s in Eq. (16), the dimensionless full Green function $g = \hbar\omega_L G$ then reads

$$g(\epsilon) = \sum_s \frac{4}{\epsilon + s\eta + \sqrt{(\epsilon + s\eta)^2 - 8cv_0^2 D}} \tag{19}$$

As it is known, the poles of the Green function contains the information of the spectral dispersion relation for the system and the lifetime of the quasiparticles. In Fig. 1, the electronic density of states can be seen for c=0.02 and different values of v_0. In turn, in the same figure the spin polarized self-energies are shown. There are two peaks around $\pm\eta$ for values of $v \to 0$ as it is expected. When the spin-polarized imaginary parts of the self-energy overlap in energy, then the density of states overlap and we obtain and the system undergoes the so-called split-band metal-insulator transition. This transition can be obtained by noting that the imaginary part of the self-energies contributes considerably to the DOS and in turn, as it was discussed above, the particular values where σ_s jumps from 0 to an small negative imaginary number is given by the condition that the argument of the third term of Eq. (18) must be less than zero. Then the band edges occurs at the critical values at which $\Im\sigma_s = 0$ and are given by

$$\epsilon_{cr} = s\eta \pm \sqrt{8cv_0^2 D} \tag{20}$$

From each spin we obtain two values for ϵ_{cr} that corresponds to the point in which σ_s crosses the horizontal axis. From those values, we are interested in the two particular values that lie near the vertical line. By substracting this values it is possible to obtain a metal-insulator diagram $c - v_0$ where an overlaping of self-energies appear. This phase is given by the equation $\sqrt{8cv_0^2 D} = \eta$, which implies that $v_0 = v_F\sqrt{\frac{2}{c}}$. In the same way we can consider the case in which Q=1. The self-consistent equation for the spin-polarized self energies reads

$$\sigma_s = cv_0^2\left[\frac{2}{\epsilon + \eta s - \sigma_s} + \frac{\epsilon + \eta s - \sigma_s}{1 - (\epsilon + \eta s - \sigma_s)^2}\right] \tag{21}$$

Last equation contains four solutions for σ_s and two of them have the desired analytical properties. In Fig. 2, the density of states is shown for c=0.02 and different values for v_0. For the lowest value of v_0 the DOS shows four remarkable peaks that are the localized states at $\epsilon = \pm\eta \pm 1$. For higher values of v_0 the gap closes between the states close to the Fermi energy and reaches the full metallic phase.

3. Magnetic oscillations for weak magnetic fields

In the case of very weak magnetic fields, we will consider that $Q \to \infty$ which implies to consider the totality of Landau levels.[4] We will restore the dimensions in order to keep track of the B dependence. The free energy is defined as $F = \Omega + \mu N$, where μ is the chemical potential, N is the number of electrons per unit area and Ω is the grand potential that reads

$$\Omega = -\frac{1}{\beta}\int_0^\infty \rho(E)\ln(1 + e^{-\beta(E-\mu)})dE \tag{22}$$

where $\rho(E)$ is the density of states in the presence of magnetic field and impurities, $\beta = 1/kT$ is the inverse temperature and μ is the chemical potential. Through the grand potential, the magnetization can be obtained as $M = -\frac{\partial\Omega}{\partial B}$. By using the general result of Eq. (16) and summing in the conduction and valence band, the density of states can be written as

$$\rho(E) = -\frac{D}{2\pi}\Im\sum_s\sum_{n=0}^{\infty}\frac{2(E - s\gamma_z B - \Sigma_s)}{(E - s\gamma_z B - \Sigma_s)^2 - \gamma_l^2 Bn} \tag{23}$$

where we have neglected the asymmetry in the sublattice population of the ground state, $D = AB/\phi_0$ is the degeneracy of each Landau level and $\gamma_z \sim 0.1\ meV/T$, $\gamma_l \sim 36\ meV/T$ in graphene. By considering the generalization of the Poisson sumation formula (see eq.(1) of [29]), the sum in n in Eq. (23) can be written as

$$\sum_{n=0}^{\infty} f_s(n) = \sum_{m=-\infty}^{\infty}\int_a^\infty f_s(x)e^{2m\pi ix}dx \tag{24}$$

where

$$f_s(x) = \frac{1}{(E - s\gamma_z B - \Sigma_s)^2 - \gamma_l^2 Bx} \tag{25}$$

and a is a number between -1 and 0. By introducing the coordinate transformation $x = t + \frac{\mu}{\gamma_l\sqrt{B}}$ and considering that $\mu \gg \gamma_l\sqrt{B}$ for weak magnetic fields, then the lower limit of integration of Eq. (24) can be replaced by $-\infty$. By applying residue theorem (see Appendix for details), the density of states can be written as

$$\rho(E) = -\frac{2D}{\gamma_l^2 B}\Im\sum_s i(E - s\gamma_z B - \Sigma_s)\left[1 + 2\sum_{m=1}^{\infty}\cos\left[\frac{2m\pi}{\gamma_l^2 B}(E - s\gamma_z B - \Sigma_s)^2\right]\right] \tag{26}$$

By integrating by parts Eq. (22), the grand potential can be written as

[4] We will not consider spin mixing levels in the energy, although we have study the phenomena in [28].

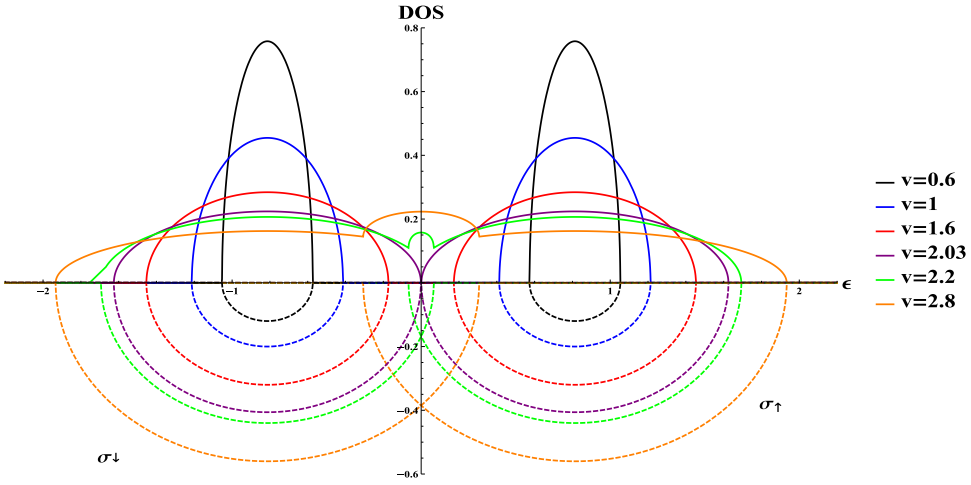

Fig. 1. Left: Density of states and imaginary part of self-energy for the K valley and different values of v_0 and where c=0.02 for B such that Q=0.

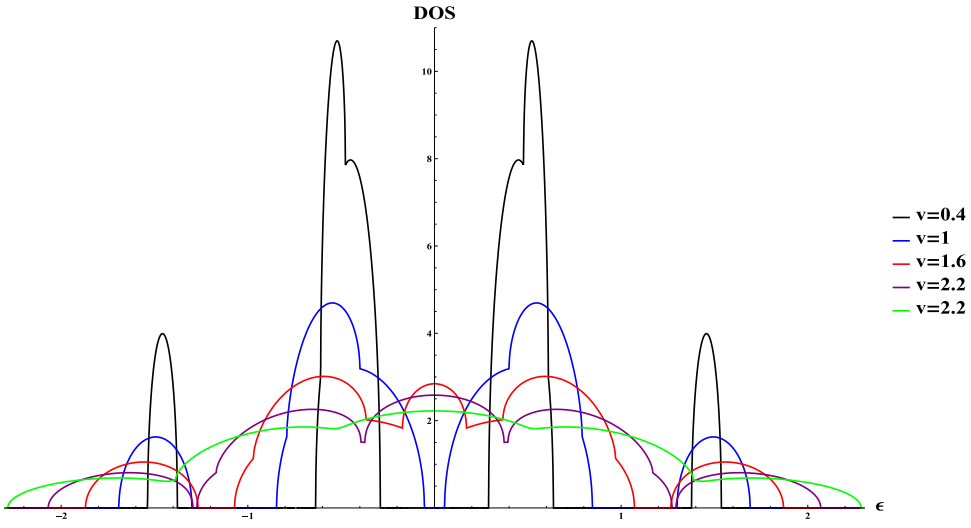

Fig. 2. Left: Density of states for the K valley and different values of v_0 and where c=0.02 for B such that Q=1.

$\Omega = -\int_0^\infty n(E)f(E)dE$, where $n(E)$ is the integrated density of states and $f(E)$ is the Fermi-dirac distribution

$$n(E) = \int_0^E \rho(E)dE \qquad f(E) = \frac{1}{1+e^{\beta(E-\mu)}} \tag{27}$$

By applying the Sommerfeld expansion for low temperatures, the thermodynamical potential reads

$$\Omega = -\int_0^\infty n(E)f(E)dE = -\int_0^\mu n(E)dE - \frac{\pi^2}{6\beta^2}\rho(\mu) + O(\beta^{-4}) \tag{28}$$

For the sake of simplicity we will assume that Σ_s does not depend on E, then the function $n(E)$ reads

$$n(E) = -\frac{2D}{\gamma_l^2 B}\sum_s \left(\frac{1}{2}E - s\gamma_z B - \Sigma_s\right)E - \tag{29}$$

$$D\sum_s\sum_{m=1}^\infty \frac{1}{2\,m\pi}\left[\sin\left[\frac{2\,m\pi}{\gamma_l^2 B}(E - s\gamma_z B - \Sigma_s)^2\right] - \sin\left[\frac{2\,m\pi}{\gamma_l^2 B}(\Sigma_s - s\gamma_z B)^2\right]\right]$$

Performing the integration

$$\int_0^\mu n(E)dE = -\frac{2D}{\gamma_l^2 B}\left[\frac{\mu^3}{3} - \frac{\mu^2}{2}(\Sigma_+ + \Sigma_-)\right] - \tag{30}$$

$$D\sum_s\sum_{m=1}^\infty \frac{1}{2\,m\pi}\left[\sqrt{\frac{\gamma_l^2 B}{m}}\,\Delta S_s(\mu, B, m) - \mu\sin\left[\frac{2\,m\pi}{\gamma_l^2 B}(-s\gamma_z B + \Sigma_s)^2\right]\right]$$

where

$$\Delta S_s(\mu, B, m) = S\left[\sqrt{\frac{m}{\gamma_l^2 B}}\,(\mu - 2(\Sigma_s - s\gamma_z B))\right] - S\left[\sqrt{\frac{4\,m}{\gamma_l^2 B}}\,(\Sigma_s - s\gamma_z B)\right] \tag{31}$$

where $S[x]$ is the Fresnel integral. Using that $M = -\frac{\partial\Omega}{\partial B}$, from Eq. (30), the total magnetic oscillations at T=0 reads

$$M = M_{osc}^{(0)}(B) + BM_{osc}^{(1)}(B) \tag{32}$$

where

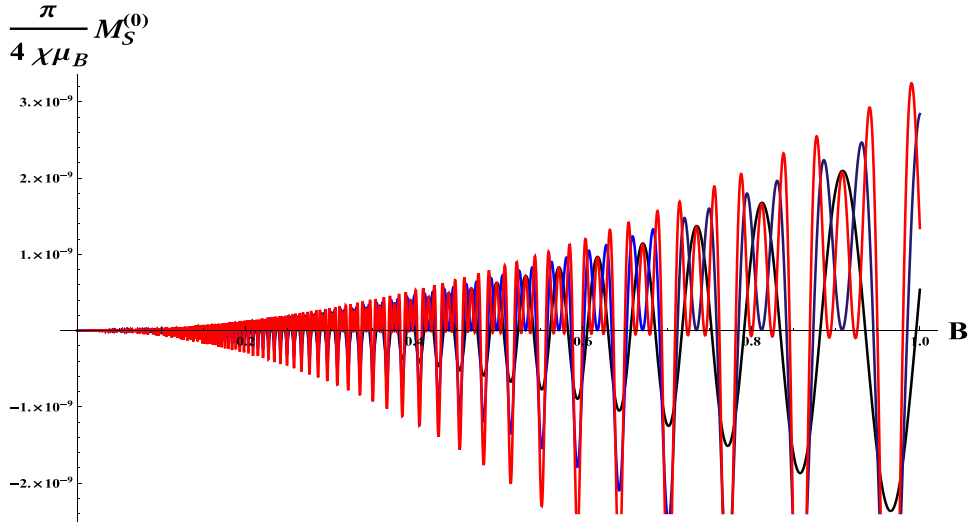

Fig. 3. Total magnetization without disorder for $\mu = 0.1\,eV$ and different contributions of modes m.

$$M_{osc}^{(0)}(B) = \frac{A}{\phi_0}\sum_s\sum_{m=1}^{\infty}\frac{1}{2\,m\pi}\left[\sqrt{\frac{\gamma_l^2 B}{m}}\,\Delta S_s(\mu, B, m) - \mu\sin[\frac{2\,m\pi}{\gamma_l^2 B}(-s\gamma_z B + \Sigma_s)^2]\right] \tag{33}$$

and

$$M_{osc}^{(1)}(B) = D\frac{\partial}{\partial B}\left(\sum_s\sum_{m=1}^{\infty}\frac{1}{2\,m\pi}\left[\sqrt{\frac{\gamma_l^2 B}{m}}\,\Delta S_s(\mu, B, m) - \mu\sin\left[\frac{2\,m\pi}{\gamma_l^2 B}(-s\gamma_z B + \Sigma_s)^2\right]\right]\right) \tag{34}$$

where the first term in Eq. (30) do not contributes to the magnetization because D/B do not depends on B. The oscillations do not have a constant frequency when the Zeeman effect and disorder are turned on. With no disorder and $\mu = 0$, the frequencies involved in the oscillations are $\omega_m = \frac{2\pi m\gamma_z^2}{\gamma_l^2} \sim (4\times 10^{-5})m$ with constant period in B. Without Zeeman effect the oscillations shows a period with $1/B$ as $\frac{2\,m\pi\mu^2}{\gamma_l^2}$ in concordance with the B^{-1} Onsager relation for the period.

In turn, we can compute the Pauli magnetization $M_S = \mu_B(n_+ - n_-)$, where $n_\pm = \int_0^\mu \rho_\pm(E)dE$ are the spin populations and μ_B is the Bohr magneton

$$M_S = \mu_B(M_S^{(0)} + M_S^{(osc)}) \tag{35}$$

where

$$M_S^{(0)} = \frac{2D\mu}{\gamma_l^2 B}[2\gamma_z B + \Sigma_- - \Sigma_+] \tag{36}$$

and

$$M_S^{(osc)} = D\sum_{s=\pm 1}\sum_{m=1}^{\infty}\frac{s}{2\,m\pi}\left[\sin\left[\frac{2\,m\pi}{\gamma_l^2 B}(\mu + s\gamma_z B - \Sigma_s)^2\right] - \sin\left[\frac{2\,m\pi}{\gamma_l^2 B}(s\gamma_z B - \Sigma_s)^2\right]\right] \tag{37}$$

Without disorder we have

$$\frac{1}{\mu_B}M_S(\Sigma = 0) = \frac{4D\gamma_z\mu}{\gamma_l^2} - D\sum_{m=1}^{\infty}\frac{1}{2\,m\pi}\left[\sin\left[\frac{2\,m\pi}{\gamma_l^2 B}(\gamma_z B - \mu)^2\right] - \sin\left[\frac{2\,m\pi}{\gamma_l^2 B}(\gamma_z B + \mu)^2\right]\right] \tag{38}$$

In Fig. 3, the oscillating contribution $M_{osc}(B)$ without disorder is plotted as a function of B for $\mu = 0.1\,eV$ and increasing number of modes m.[5] These theoretical are in concordance with the results reported for epitaxial monolayer in graphene by [30] that cannot account for the oscillations for small values of B. The sharp sawtooth-like oscillating behavior of magnetization in graphene (see [31]) is reached taking into account higher modes contributions. In turn, from last equation it can be seen that two sine functions with different arguments contributes. By rearranging the terms, the oscillating part can be written as

$$\sin\left[\frac{2\,m\pi}{\gamma_l^2 B}(\gamma_z B - \mu)^2\right] - \sin\left[\frac{2\,m\pi}{\gamma_l^2 B}(\gamma_z B + \mu)^2\right] = -2\cos\left[\frac{2\,m\pi}{\gamma_l^2 B}(\gamma_z^2 B^2 + \mu^2)\right]\sin\left(\frac{4\,m\pi\gamma_z\mu}{\gamma_l^2}\right) \tag{39}$$

Last result implies that magnetic oscillations are modulated by a beat frequency that does not depend on B and depends exclusively with μ.

3.1. Self–energy contribution

In order to compute the contribution from the energy dependent self-energy in the magnetic oscillations we can consider the Born approximation $\Sigma^{NSCBA}(z) = cV_0^2\sum_k G_0(k)$ where G_0 is the bare Green function with no disorder. Applying the Poisson summation formula in Eq. (14), the self-energy equation reads

$$\Sigma_s(E) = \frac{2cV_0^2 D}{\gamma_l^2 B}(E - s\gamma_z B)\left[1 + 2\sum_{m=1}^{\infty}\cos\left[\frac{2\,m\pi}{\gamma_l^2 B}(E - s\gamma_z B)^2\right]\right] \tag{40}$$

For the sake of simplicity we can consider the non-oscillatory part.

[5] We are using that $\mu = \epsilon_F \sim 0.1\,eV$ as a first approximation for the chemical potential, where we are neglecting the oscillating part of μ. The second oscillating term of the chemical potential represent a small correction to the constant value of chemical potential.

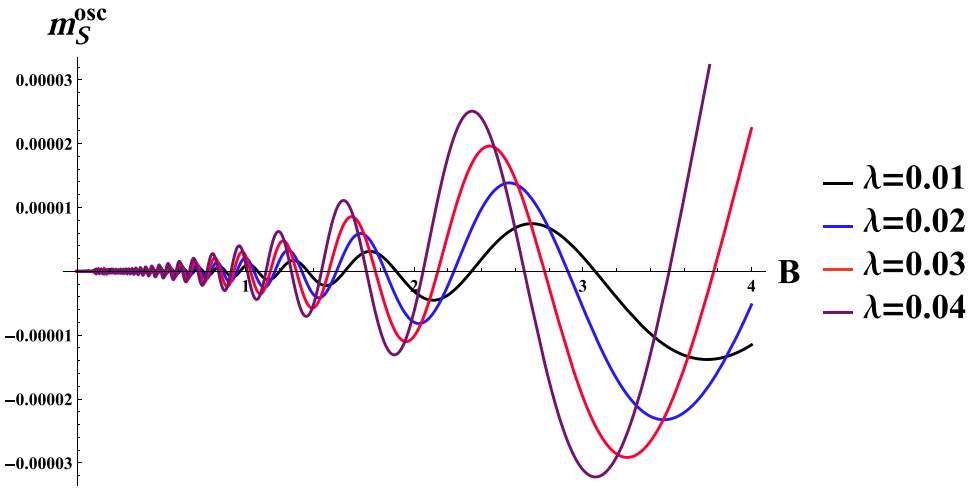

Fig. 4. Spin magnetization for $\mu = 0.1\ eV$ and different values of $\lambda = \frac{2cV_0^2\kappa}{\gamma_l^2}$.

Then

$$\Sigma_s^{(no)} = \frac{2cV_0^2 D}{\gamma_l^2 B}(E - s\gamma_z B) \tag{41}$$

With this self-energy, Eq. (26) reads

$$\rho(E) = -\frac{2D}{\gamma_l^2 B}\sum_s (E - s\gamma_z B)\left(1 - \frac{2cV_0^2 D}{\gamma_l^2 B}\right) \left[1 + 2\sum_{m=1}^{\infty}\cos\left[\frac{2\,m\pi}{\gamma_l^2 B}(E - s\gamma_z B)^2\left(1 - \frac{2cV_0^2 D}{\gamma_l^2 B}\right)^2\right]\right] \tag{42}$$

This result is identical to the case $\Sigma_s = 0$ but with the renormalized energy $E - s\gamma_z B \to \chi(E - s\gamma_z B)$, where $\chi_{imp} = 1 - \lambda$ where $\lambda = \frac{2cV_0^2\kappa}{\gamma_l^2}$ and $\kappa = \frac{A}{\phi_0}$. The frequency of oscillations is

$$\omega_m^{(s)} = \frac{2\,m\pi}{\gamma_l^2 B}\chi_{imp}^2(\mu - s\gamma_z B)^2 \tag{43}$$

and the spin magnetization reads

$$\frac{1}{\mu_B}M_S = \frac{4\kappa\gamma_z\mu}{\gamma_l^2}[1 + \lambda] - m_S^{osc} \tag{44}$$

where

$$m_S^{osc} = D\sum_{s=\pm 1}\sum_{m=1}^{\infty}\frac{s}{2\,m\pi}\left[\sin\left[\frac{2\,m\pi}{\gamma_l^2 B}(\mu(1-\lambda) + s\gamma_z B(1+\lambda))^2\right] - \sin\left[\frac{2\,m\pi}{\gamma_l^2 B}(s\gamma_z B(1+\lambda) - \lambda\mu)^2\right]\right] \tag{45}$$

without Zeeman effect, the magnetic oscillations behaves as $\frac{2\,m\pi\mu^2}{\gamma_l^2 B}(1-\lambda)^2$. In Fig. 4, the oscillating part of the spin magnetization is shown for different values of λ. The value $\mu = 0.1\ eV$ has been used for the chemical potential. As B increases, the amplitude of the dHvA oscillations is fixed in a constant non-zero value $\frac{4\kappa\gamma_z\mu}{\gamma_l^2}[1+\lambda]$, which is a different behavior of those obtained in conventional semiconductor 2DEG, where it is well known that the oscillating center of the magnetization remains exactly at zero. This difference can be atributed to the reduced diamagnetic contribution on the magnetization in graphene with respect to conventional semiconductors (see [16]). In this case, althought the numerical calculations have been done for lower values of B, the differences in the maximum and minimum of the oscillations are in the order of 10^{-5} eV. The linear behavior of the oscillations in the magnetization is a consequence of the Zeeman effect, which splits the dHvA oscillations in a magnitude of the order of the Zeeman energy. The results obtained are similar to those found for magnetoresistance oscillations in different systems (see [32]). By applying Fourier transform on the magnetization obtained in Fig. 4, the main peak is around $\omega \sim 4\,T^{-1}$ which gives a fundamental magnetic field $f(T) \sim (\frac{\omega}{2\pi})^{-1} \sim 4\,T$ which is in the order of the results obtained in [33] for graphite. In Fig. 3 the Zeeman energy and the pseudospin-Landau coupling effects are present: the latter by decreasing the Fermi level and introducing the magnetic oscillations and the former by splitting these oscillations for both spins.[6] The deformation of the Fermi surface due to the impurities introduces new electron orbits with small periods and in consequence, higher frequencies. These new closed orbits appear as higher harmonics in the magnetic oscillations. By applying Fourier transform to the magnetic oscillations, these new frequencies can be obtained and the respective periods. Then, it is possible to reconstruct the deformed Fermi surface. If we consider only one spin, the density of states and the Fermi level induces dHvA oscillations, which reflects the closed orbits in the Fermi surface. When both spins are taking into account, the minimal differences between the dHvA oscillations for each spin are enhanced in the total magnetization due to the Zeeman splitting. In this sense, the magnetization due to the Zeeman splitting can be interpreted as a fine tuning of the dHvA oscillations that intensify the effects of the impurities in the electronic density of states and can be used experimentally to obtain a detailed information about the Fermi surfaces involved in the magnetic oscillations. A particular case of impurities is when $V \to -\infty$, which is the case of vacancies. In [22], the case of vacancies is considered in detail, where by using Eq. (16) and Eq. (18) of this paper, the Green function with a finite small density of vacancies $n_v = N_v/N$, where N_v is the number of vacancies and N the number of carbon atoms, reads

$$\langle G(\alpha, s, n, k, z)\rangle = [G_0^{-1}(\alpha, s, n, k, z) + n_v G_{0\,s}^{-1}(z)]^{-1} \tag{46}$$

where $G_{0\,s}(z) = \int\frac{dk}{2\pi}\sum_{\alpha=\pm 1}\sum_{n=0}^{Q} G_0(\alpha, s, n, k, z)$ is the integrated clean Green function. Then, Eq. (2) contains the term $n_v G_0^{-1}(z)$ that can be considered a complex number. In this sense, the Green function with vacancies is identical to consider that the self-energy $\Sigma_s(z)$ can be written as $\Sigma_s(z) = -n_v G_{0\,s}^{-1}(z)$. In fact, this can be seen by comparing eq. (2) with Eq. (10). Then, all the machinery used to compute the magnetization with self-energy included can applied for the case of vacancies. In particular, we have computed the density of states for an arbitrary self-energy (see Eq. (26)). To compute $\Sigma_s(z) = -n_v G_{0\,s}^{-1}(z)$, we

[6] In different systems, the crossover between Zeeman effect and Rashba coupling has been studied (see [34]).

can apply Poisson sumation formula as it was done in eq. (40) to $G_{0\,s}(z)$. The non-oscillatory part of $G_{0\,s}(z)$ reads

$$G_{0\,s}^{(no)}(E) = \frac{4D}{\gamma_l^2 B}(E - s\gamma_Z B) \tag{47}$$

then the non-oscillatory part of the self-energy reads

$$\Sigma_s^{(no)}(E) = -\frac{\gamma_l^2 n_v}{4\kappa(E - s\gamma_Z B)} \tag{48}$$

which is different from result of Eq. (41) for the non-oscillatory part of the self-energy in the case of impurities. In this case, in order to obtain $n_s(\mu)$ we must integrate $\rho(E)$, but the dependence in E is not simple as in the case of impurities. For B=0, the density of states is singular in the low-frequency regime. We consider that the vacancy case deserves a deep study in order to compare the results with the magnetic oscillations with impurities. Nevertheless, we can study the behavior of the spin magnetic oscillations near the singularity. For this we have to consider the density of states near the singularity, then we can approximate $E - s\gamma_z B - \Sigma_s = E - s\gamma_z B + \frac{\gamma_l^2 n_v}{4\kappa(E - s\gamma_Z B)} \sim \frac{\gamma_l^2 n_v}{4\kappa(E - s\gamma_Z B)}$ for $E - s\gamma_Z B \to 0$. Considering this we can compute the integral of the density of states and the spin magnetization

$$m_s^{vac} = n_v \ln\left(\frac{\gamma_z B - \mu}{\gamma_z B + \mu}\right) + n_v \sum_{m=1}^{\infty}\left[Ci\left(\frac{\gamma_l^2 n_v^2 m\pi}{2B\kappa^2(\mu + \gamma_z B)^2}\right) - Ci\left(\frac{\gamma_l^2 n_v^2 m\pi}{2B\kappa^2(\mu - \gamma_z B)^2}\right)\right] \tag{49}$$

where $Ci(x)$ is cosine integral. The argument of the sinusoidal functions reads

$$\omega_m^{vac} = \frac{\gamma_l^2 n_v^2 m\pi}{2B\kappa^2(\mu \pm \gamma_z B)^2} \tag{50}$$

which only in the case of vanishing Zeeman effect behaves as B^{-1}.

These effects could be detected for the specific configurations considered in this work, although other effects must be taken into account for the final result such as intrinsic and extrinsic Rashba-orbit couplings and magnetic moments originated by the orbital angular momentum (see [35]) or temperature effects in the dHvA oscillations (see [36]). From the experimental viewpoint, doping in graphene can be obtained through electric doping by changing gate voltage (see [37]) or by chemical doping, which is discussed as surface transfer doping and subtitutional doping (see [38]). For a general review of the experimental procedure to obtain doping asymmetry in graphene see [39] and the references therein and for the direct experimental determination of the chemical bonding of individual impurity atoms see [40]. In the case that p-type and n-type doping can be achieved in a controlled way and where the experimental determination of the on-site energies results in slightly different values, then it would be possible to tune up population difference in both spins due to the Zeeman effect. It has been shown that the Zeeman splitting can be controlled by the strength of the magnetic field in the topological cones with long range Coulomb impurities (see [41]).

4. Conclusions

In this work we have reported a theoretical study on the modulation of de Haas-van Alphen effect in graphene by magnetic field taking into account the Zeeman effect. The electronic properties of doped graphene have been computed using the Born approximation for the self-energy. The de Haas van Alphen oscillations have been found for each spin using the Poisson summation formula. At the zero temperature, the magnetization are predicted to oscillate periodically as a function of reciprocal field $1/B$ when there is no disorder and no Zeeman effect. When the Zeeman effect is considered, the oscillations changes and the period become B dependent and the Onsager relation is recovered for half-filling. In turn, the Pauli magnetization is computed by taking into account the shift introduced in the electronic density of states due to the Zeeman splitting and spin population. By combining this effect with the dHvA oscillations, it is shown how the total magnetization increases linearly for small values of B and the oscillations are on the order of the Zeeman energy. In turn, a beat frequency modulates the dHvA oscillations that depends linearly with the chemical potential. When impurities are introduced randomly, Landau levels are broadening and the frequency of the magnetic oscillations do not obey the Onsager relation and depends quadratically with B. These effects are enhanced in the Pauli magnetization and can be used to determine the Fermi surface of low dimensional systems with impurities. These phenomena, not available in the standard 2D electron gas, are a consequence of the relativistic type spectrum of low energy electrons and holes in graphene.

Author contributions

All authors contributed equally to all aspects of this work.

Acknowledgment

This paper was partially supported by grants of CONICET (Argentina National Research Council) and Universidad Nacional del Sur (UNS) and by ANPCyT through PICT 1770, and PIP-CONICET Nos. 114-200901-00272 and 114-200901-00068 research grants, as well as by SGCyT-UNS., A.J., P.V.J. J. S. A. are members of CONICET. F. E. is a fellow researcher at this institution.

Appendix A. Appendix

In order to solve the density of states $\rho(E)$ we can sum over the conduction and valence band as it was shown in Eq. (23).

$$\rho(E) = -\frac{D}{\pi}\Im\sum_s\sum_{n=0}^{\infty}\frac{2(E - s\gamma_z B - \Sigma_s)}{(E - s\gamma_z B - \Sigma_s)^2 - \gamma_l^2 Bn} \tag{51}$$

By using the Poisson summation formula and introducing the coordinate transformation $x = t + \frac{\mu^2}{\gamma_l^2 B}$ and considering that $\mu \gg \gamma_l\sqrt{B}$ for weak magnetic fields, then the lower limit of integration in the Poisson summation formula can be replaced by $-\infty$, then

$$\sum_{n=0}^{\infty} f_s(n) = \frac{1}{\gamma_l^2 B}\sum_{m=-\infty}^{\infty} e^{-2m\pi i\frac{\mu^2}{\gamma_l^2 B}}\int_{-\infty}^{\infty}\frac{e^{2m\pi i t}}{\frac{(E - s\gamma_z B - \Sigma_s)^2}{\gamma_l^2 B} - t - \frac{\mu^2}{\gamma_l^2 B}}dt \tag{52}$$

Last equation can be solved using residue theorem, where the pole reads

$$t_0 = a_0 + \frac{\mu^2}{\gamma_l^2 B} - ib_0 \tag{53}$$

where

$$a_0 = \frac{1}{\gamma_l^2 B}[(E - s\gamma_z B - \Re\Sigma_s)^2 - \Im^2\Sigma_s] \tag{54}$$

$$b_0 = \frac{1}{\gamma_l^2 B}\Im\Sigma_s(E - s\gamma_z B - \Re\Sigma_s)$$

where the imaginary part of the pole is located in the upper or lower half plane given the sign of $\Im\Sigma_s$. Then, by closing the contour, Eq. (52) reads

$$\sum_{n=0}^{\infty} f_s(n) = \frac{2\pi i}{\gamma_l^2 B}\sum_{m=-\infty}^{\infty}[\theta(\Im\Sigma_s)e^{2\,m\pi i(a_0-ib_0)} + \theta(-\Im\Sigma_s)e^{2\,m\pi i(a_0+ib_0)}] \tag{55}$$

$$= \frac{2\pi i}{\gamma_l^2 B} + \frac{4\pi i}{\gamma_l^2 B}\sum_{m=1}^{\infty}[\theta(\Im\Sigma_s)\cos[2\,m\pi(a_0 - ib_0)] + \theta(-\Im\Sigma_s)\cos[2\,m\pi(a_0 + ib_0)]$$

where the integral in the semicircle Γ of radius R vanishes for $R \to \infty$. With this result, the density of states reads

$$\rho(E) = -\frac{2D}{\gamma_l^2 B}\Im\sum_s i(E - s\gamma_z B - \Sigma_s)\times \tag{56}$$

$$\left[1 + 2\sum_{m=1}^{\infty}[\theta(\Im\Sigma_s)\cos[2\,m\pi(a_0 - ib_0)] + \theta(-\Im\Sigma_s)\cos[2\,m\pi(a_0 + ib_0)]\right]$$

For simplicity, in Section 2 we will consider that $\Im\Sigma_s < 0$, then we have to consider only the first term in the sum in m.

References

[1] K.S. Novoselov, A.K. Geim, S.V. Morozov, D. Jiang, M.I. Katsnelson, I.V. Grigorieva, S.V. Dubonos, A.A. Firsov, Nature 438 (2005) 197.
[2] A.K. Geim, K.S. Novoselov, Nat. Mater. 6 (2007) 183.
[3] A.H. Castro Neto, F. Guinea, N.M.R. Peres, K.S. Novoselov, A.K. Geim, Rev. Mod. Phys. 81 (2009) 109.
[4] P.R. Wallace, Phys. Rev. 71 (1946) 9.
[5] Ganhua Lu, Kehan Yu, Zhenhai Wena, Junhong Chen, Nanoscale 5 (2013) 1353–1368.
[6] S. Kuru, J. Negro, L.M. Nieto, J. Phys.: Condens. Matter 21 (2009) 455305.
[7] K.S. Novoselov, Z. Jiang, Y. Zhang, S.V. Morozov, H.L. Stormer, U. Zeitler, J.C. Maan, G.S. Boebinger, P. Kim, A.K. Geim, Science 315 (2007) 5817.
[8] J.S. Ardenghi, P. Bechthold, P. Jasen, E. Gonzalez, O. Nagel, Phys. B 427 (2013) 97–105.
[9] V.P. Gusynin, S.G. Sharapov, Phys. Rev. Lett. 95 (2005) 146801.
[10] W. de Haas, P. van Alphen, Proc. Acad. Sci. Amst. 33 (1930) 1106–1118.
[11] D. Shoenberg, Philos. Trans. R. Soc. Lond. 245 (1952) 1–57.
[12] L. Onsager, Mag. J. Sci.: Ser. 7 (43) (1952) 344.
[13] I. Meinel, T. Hengstmann, D. Grundler, D. Heitmann, W. Wegscheider, M. Bichler, Phys. Rev. Lett. 82 (1999) 819.
[14] S.G. Sharapov, V.P. Gusynin, H. Beck, Phys. Rev. B 69 (2004) 075104.
[15] T. Champel, V.P. Mineev, Philos. Mag. B 81 (2001) 55.
[16] F. Zhen-Guo, W. Zhi-Gang, L. Shu-Shen, Z. Ping, Chin. Phys. B 20 (5) (2011) 058103.
[17] S. Uji, J.S. Brooks, Y. Iye, Physica B 246–247 (1998) 299.
[18] Z.M. Wang, Q.Y. Xu, G. Ni, Y.W. Du, Phys. Lett. A 314 (2003) 328.
[19] S.V. Morozov, K.S. Novoselov, M.I. Katsnelson, F. Schedin, L.A. Ponomarenko, D. Jiang, A.K. Geim, Phys. Rev. Lett. 97 (2006) 016801.
[20] R.E. Prange, in The Quantum Hall Effect, edited by R.E. Prange and S.M. Girvin, Springer-Verlag, New York, 1987.
[21] J.S. Ardenghi, P. Bechthold, E. Gonzalez, P. Jasen, A. Juan, Eur. Phys. J. B 88 (47) (2015).
[22] N.M.R. Peres, F. Guinea, A.H. Castro Neto, Phys. Rev. B 73 (2006) 125411.
[23] F. Escudero, L. Sourrouille, J.S. Ardenghi, P. Jasen, Superlattices Microstruct. 101 (2017) 537–546.
[24] J. Rammer, Quantum Transport Theory, Perseus books, Reading, MA, 1998.
[25] S. Das Sarma, S. Adam, E.H. Hwang, E. Rossi, Rev. Mod. Phys. 83 (2011) 407.
[26] M.O. Goerbig, R. Moessner, B. Doucot, Phys. Rev. B 74 (2006) 161407.
[27] V. Janis, V. Pokorny, Phys. Rev. B 90 (2014) 045143.
[28] F. Escudero, J.S. Ardenghi, L. Sourrouille, P. Jasen, J. Magn. Magn. Mater. 429 (2017) 294–298.
[29] B.J.B. Crowley, J. Phys. A: Math. Gen. 12 (11) (1979).
[30] J. Jobst, D. Waldmann, F. Speck, R. Hirner, D.K. Maude, T. Seyller, H.B. Weber, Phys. Rev. B 81 (2010) 195434.
[31] I.A. Luk'yanchuk, Low Temp. Phys. 37 (2011) 45.
[32] J. Singleton, Rep. Progress. Phys. 63 (2000) 1111.
[33] S.B. Hubbard, T.J. Kershaw, A. Usher, A.K. Savchenko, A. Shytov, Phys. Rev. B 83 (2011) 035122.
[34] T.Y. Kim, S. Joo, J. Lee, J.H. Suh, S. Cho, S.U. Kim, K. Rhie, J. Hong, J. Korean Phys. Soc. 54 (2) (2009) 697–702.
[35] J. Luo, J. Magn. Magn. Mater. 366 (2014) 28–32.
[36] L.S. Paixão, Z.Z. Alisultanov, M.S. Reis, J. Magn. Magn. Mater. 368 (2014) 374–378.
[37] K.S. Novoselov, A.K. Geim, S.V. Morozov, D. Jiang, Y. Zhang, S.V. Dubonos, I.V. Grigorieva, A.A. Firsov, Science 306 (2004) 666.
[38] C.N.R. Rao, A.K. Sood, K.S. Subrahmanyam, A. Govindaraj, Angew. Chem. 48 (2009) 7752.
[39] H. Liu, Y. Liu, D. Zhua, J. Mater. Chem. 21 (2011) 3335–3345.
[40] W. Zhou, M.D. Kapetanakis, M.P. Prange, S.T. Pantelides, Phys. Rev. Lett. 109 (2012) 206803.
[41] B.S. Kandemir, D. Akay, J. Magn. Magn. Mater. 384 (2015) 101–105.